Influence of *N*-Substitution on the Formation and Oxidation of NHC−CAAC-Derived Triazaalkenes

Debdeep Mandal,[†] Ramapada Dolai,[†] Ravi Kumar,[‡] Simon Suhr,[§] Nicolas Chrysochos,[‖]
Pankaj Kalita,[⊥] Ramakirushnan Suriya Narayanan,[†] Gopalan Rajaraman,*,[‡] Carola Schulzke,*,[‖]
Biprajit Sarkar,*,[§] Vadapalli Chandrasekhar,*,[†,#] and Anukul Jana*,[†]

[†]Tata Institute of Fundamental Research Hyderabad, Gopanpally, Hyderabad 500107, India

[‡]Department of Chemistry, Indian Institute of Technology Bombay, Powai, Mumbai 400076, India

[§]Institut für Chemie und Biochemie, Anorganische Chemie, Freie Universität Berlin, Fabeckstraße 34−36, Berlin 14195, Germany

[‖]Institut für Biochemie, Universität Greifswald, Felix-Hausdorff-Straße 4, Greifswald D-17487, Germany

[⊥]School of Chemical Sciences, National Institute of Science Education and Research, HBNI, Bhimpur-Padanpur, Jatni, Khurda, Bhubaneswar 752050, Odisha, India

[#]Department of Chemistry, Indian Institute of Technology Kanpur, Kanpur 208016, India

S *Supporting Information*
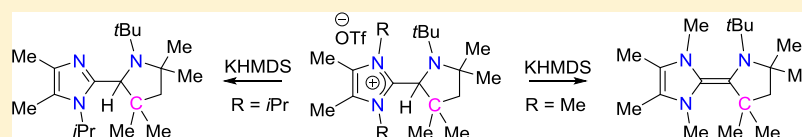
ABSTRACT: We have studied the effect of *N*-substitution on the course of the reaction of imidazolium triflate. The reaction of *N*-heterocyclic carbene with *N*-*t*Bu-substituted pyrrolinium triflate afforded 2-(pyrrolidin-2-yl)-imidazolium triflate, 3^R. Treatment of 3^R with potassium bis(trimethylsilyl)amide (KHMDS) leads to either the dealkylation product **4** or the deprotonation product, triazaalkene **5**, depending on the *N*-substitution at the imidazolium moiety. Density functional studies using the B3LYP/TZVP setup have been employed to explore various pathways for the dealkylation reaction and the calculated energies support the dealkylation by a large energy margin compared to the deprotonatation process. Theoretical calculations revealed that dealkylation reaction is thermodynamically more favorable than deprotonation. The triazaalkene **5** could be oxidized by AgOTf to the corresponding radical cation **6** and dication **7** in-situ. While **6** and **7** could not be isolated, the formation of the former is inferred by electron paramagnetic resonance spectroscopy and its abstraction of a H-atom to afford 3^{Me}. Similarly, the formation of the dication **7** is inferred by its ready elimination of isobutylene affording **8**.

1. INTRODUCTION

In recent years, the chemistry of cyclic(alkyl)(amino)-carbenes, CAACs has expanded in parallel to that of the more traditional *N*-heterocyclic carbenes (NHC), NHCs.[1] Because of the different electronic situation at the carbenic centre of NHC and CAAC, there is a remarkable difference in the chemistry of these two families, which is strikingly visible in their organic chemistry,[2] main group chemistry,[3] and organometallic chemistry.[4] As a new development of CAAC chemistry, the combination of NHC and CAAC has resulted in the synthesis of electron-rich triazaalkenes with three isolable oxidation states.[5] An aspect of the NHC chemistry that needs to be emulated in CAAC chemistry is the striking reactivity differences that are present in the former by variation in *N*-substituents: aryl[6] versus alkyl.[7] One of the notable examples of this reactivity difference is demonstrated in the isolation of silicon(II)-dihalides, Si(II)X$_2$ (X = Cl, Br, and I), **I** when *N*-2,6-diisopropylphenyl-substituted NHC is used (Scheme 1).[8] On the other hand, use of a *N*-methyl-substituted NHC, a sterically less-hindered

Scheme 1. Chemical Structures of I and II (Dip = 2,6-*i*Pr$_2$C$_6$H$_3$)
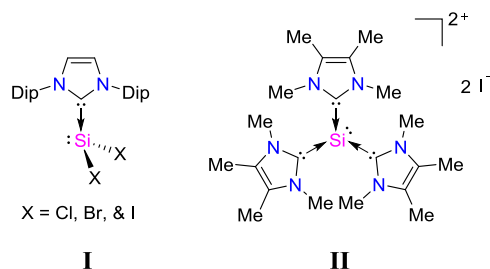
donor center, allows the stabilization and isolation of the dicationic Si(II)-complex, **II** by multiple NHC coordination to the silicon centre (Scheme 1).[9]

In a further demonstration of this intriguing reactivity variation upon change of *N*-substituents, recently, we

reported the reaction of *N*-alkyl-substituted NHC, **1**[R] with *N*-isopropyl-substituted pyrrolinium cation, **2**[iPr] leading to the formation of 2-(pyrrolidin-2-yl)-imidazolium cation, **III**[5c] (Scheme 2). From these 2-(pyrrolidin-2-yl)-imidazolium

Scheme 2. Reaction of *N*-Alkyl NHC with Conjugate Acid of *N-i*Pr CAAC
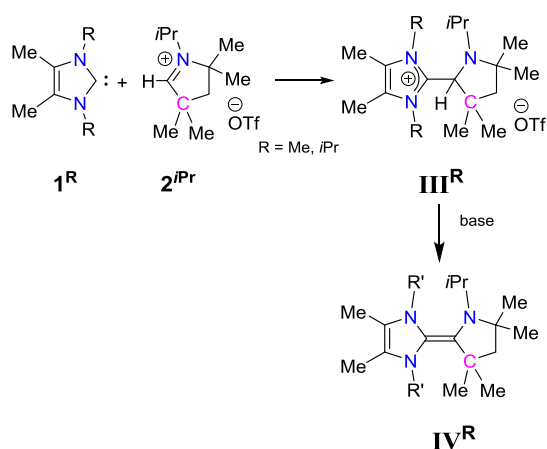
cations *N*-peralkyl-substituted CAAC−NHC-based triazaole-fins, **IV** have been isolated through deprotonation (Scheme 2). The electron oxidation of these triazaolefins gave radical cations and dications which are isolable in nature.

On the other hand, we observed the "abnormal" addition of *N*-aryl-substituted NHC, **V** with conjugate acid of CAAC, **2**[R] under the formation of 4-(pyrrolidin-2-yl)-imidazolium cation, **VI**[R] (Scheme 3).[10] Mechanistic study revealed that

Scheme 3. Reaction of NHC[Dip] **(Dip = 2,6-*i*Pr$_2$C$_6$H$_3$) with Conjugate Acid of *N-i*Pr CAAC**
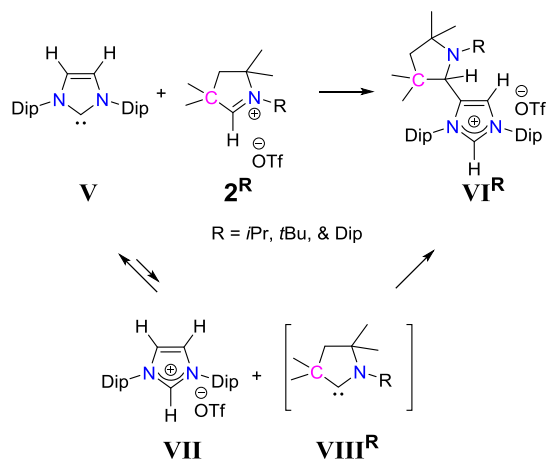
compound, **VI** is formed through an acid-base reaction between **V** and **2**[iPr], that leads to the formation of 1,3-(2,6-*i*Pr$_2$C$_6$H$_3$)-imidazolium cation, **VII** and free CAAC, **VIII**[R]. This free CAAC then underwent an oxidative addition across the C4−H centre of 1,3-(2,6-*i*Pr$_2$C$_6$H$_3$)-imidazolium cation and produced **VI**[R] (Scheme 3).

2. RESULTS AND DISCUSSION

Given the limited, yet, striking reactivity differences on variation of the *N*-substituents, we considered the reaction of *N*-alkyl-substituted NHCs, **1**[Me] and **1**[iPr] with *N-t*Bu-

substituted pyrrolinium triflate, **2**[tBu] to study the substituent effects in product formation. The reaction of **1**[Me] or **1**[iPr] with **2** in tetrahydrofuran (THF) leads to the formation of **3**[Me] and **3**[iPr], respectively, as colorless solids (Scheme 4).

Scheme 4. Synthesis of 3[R]
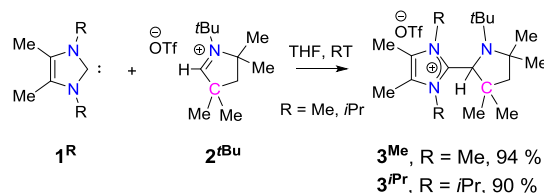
The formation of compounds **3**[Me] and **3**[iPr] were confirmed by ^{1}H NMR spectroscopy and X-ray crystallography. The ^{1}H NMR spectra of compounds **3**[Me] (δ = 4.58 ppm), and **3**[iPr] (δ = 4.72 ppm) reveal characteristic singlet peaks for the "C−H" units. These chemical shifts are considerably upfield shifted when compared with the starting cyclic iminium salt **2** (δ = 9.08 ppm).

Single crystals of **3**[Me] and **3**[iPr], suitable for XRD diffraction were grown by slow diffusion of *n*-pentane into the concentrated THF solution of **3**[Me] and **3**[iPr] at room temperature. **3**[Me] gets crystallized in a monoclinic crystal system with the $P2_1/n$ space group (Figure 1a) and **3**[iPr] gets
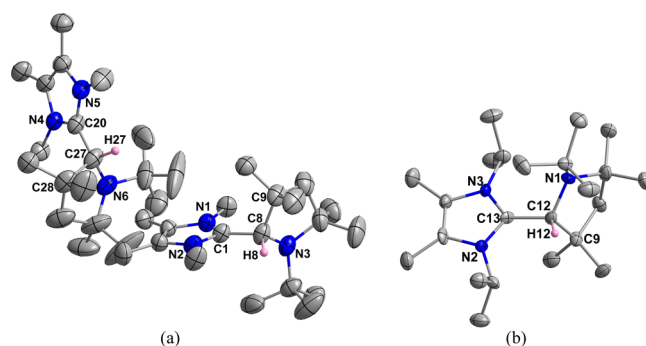
Figure 1. (a) Solid-state molecular structure of **3**[Me] (contains both the *R*- and *S*-isomers in asymmetric unit) (thermal ellipsoids at 30% probability level; triflate anion and all H atoms except C8−H8 and C27−H27 are omitted for clarity). Selected bond lengths (Å) and angles (°): C1−N1 1.326(3), C1−N2 1.335(4), C8−N3 1.463(4), C1−C8 1.517(4), C20−N4 1.334(4), C20−N5 1.338(4), C27−N6 1.459(4), C20−C27 1.510(4), N1−C1−N2 107.3(3), N3−C8−C9 107.0(3), N4−C20−N5 106.6(3), N6−C27−C28 106.2(3). (b) Solid-state molecular structure of **3**[iPr] (thermal ellipsoids at 30% probability level; triflate anion and all H atoms except C12−H12 are omitted for clarity). Selected bond lengths (Å) and angles (°): N2−C13 1.347(9), N3−C13 1.358(8), N1−C12 1.448(9), C12−C13 1.503(10), N2−C13−N3 107.0(6), N1−C12−C9 107.4(5).

crystallized in the triclinic crystal system with the $P\overline{1}$ space group (Figure 1b). Although both of these salts contained one asymmetric carbon center, only in case of **3**[Me], two enantiomers *R*- and *S*- were detected in their asymmetric units. In both of these triflate salts, the C−N bond distances of the imidazolium ring indicate delocalized double bond character, whereas the C−N bond distance in the pyrrolidine ring indicates a single bond character. Also, the central C−C bond distance indicates a single bond character.

Subsequently, 3^{iPr} and 3^{Me} were reacted with KHMDS. While the reaction with the former leads to an unprecedented *N*-dealkylation product **4**, the reaction with the latter leads to the *N*-peralkyl-substituted NHC−CAAC-based triazaolefin, **5** (Scheme 5). These results are in contrast to those of the

Scheme 5. Reactions of 3^R with KHMDS
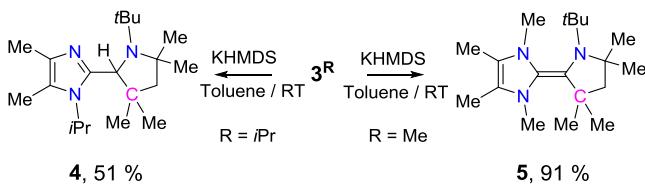
related 2-(pyrrolidin-2-yl)-imidazolium triflate with *N*-*i*Pr substitution at the pyrrolidine scaffold, where the formation of only NHC−CAAC-based triazaolefins occurred.[5c] The N−C bond cleavage of formally coordinated NHC is known for transition-metal complexes[11] and low-valent low-coordinated main group compounds.[12] Density functional theory (DFT) calculations suggest that the formation of **4** is thermodynamically favorable in comparison to the deprotonation product.[13]

The ^{1}H NMR spectrum of **4** showed a characteristic singlet and septet at $\delta = 4.15$ and $\delta = 4.25$ ppm in a 1:1 ratio for the tertiary C−H proton of the pyrrolidine moiety and the isopropyl C−H proton of the imidazole moiety, respectively. This supported the *N*-deisopropylation of the functionalized imidazolium moiety. Colorless crystals of **4** suitable for X-ray diffraction were obtained from a saturated *n*-pentane solution at −35 °C after 15 days. The C8−C9 distance in **4** is 1.503(5) Å indicating a single bond between them (Figure 2a).
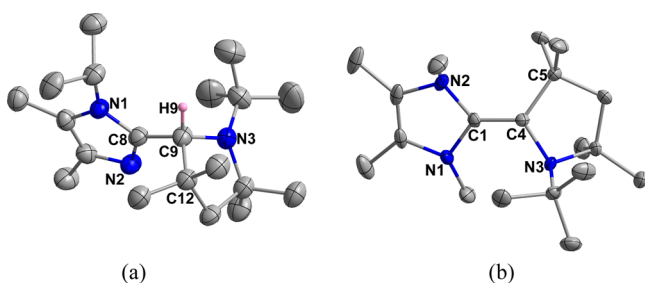
Figure 2. (a) Solid-state molecular structure of **4** (thermal ellipsoids at a 30% probability level and all H atoms except C9−H9 are omitted for clarity). Selected bond lengths (Å) and angles (°): N1−C8 1.374(4), N2−C8 1.321(4), N3−C9 1.461(4), C(8)−C(9) 1.503(5), N(2)−C(8)−N(1) 110.6(3), N(3)−C(9)−C(12) 102.5(3). (b) Solid-state molecular structure of **5** (thermal ellipsoids at a 30% probability level; the triflate anion and all H atoms are omitted for clarity). Selected bond lengths (Å) and angles (°): N1−C1 1.416(3), N2−C1.

A computational investigation using DFT has been carried out to understand the mechanism of 3^{iPr} and 3^{Me} reaction with KHMDS. We have explored all the possible pathways for 3^{iPr} and 3^{Me} reaction with the KHMDS reagent (see Scheme 6). The reagent KHMDS abstracts hydrogen from C1 carbon of 3^{iPr} and 3^{Me} to form **4′** (expected product) and **5** via transition states 3^{iPr}-**TS1a** and 3^{Me}-**TS1a**, respectively (pathway **a** for both Scheme 6a,b), while abstraction of C4 hydrogen leads to the formation of intermediates 3^{iPr}-**Int1b**

and 3^{Me}-**Int1b** via 3^{iPr}-**TS1b** and 3^{Me}-**TS1b**, which further with the transfer of the C4 hydrogen to C1 through the five-membered hydrogen-transfer cyclic transition state (3^{iPr}-**TS2b** and 3^{Me}-**TS2b**) gives **4′** and **5** (pathway **b** for both Scheme 6a,b). In case of 3^{iPr}, C5 hydrogen abstraction through the 3^{iPr}-**TS1c** leads to the formation of experimentally observed product **4** (pathway **c** of Scheme 6a). We have considered the direct attack on C4 carbon of 3^{iPr} and 3^{Me} with KHMDS (3^{iPr}-**TS1b** and 3^{Me}-**TS1b**) to give **4** and **5′** (dealkylated product) (pathway **d** Scheme 6a and pathway **c** Scheme 6b).

The 3^{iPr} reacts with KHMDS to give the expected alkene product **4′** by means of direct hydrogen abstraction from C1 carbon (3^{iPr}-**TS1a**) and has a barrier height of 216.1 kJ/mol while the C4 hydrogen abstraction transition state (3^{iPr}-**TS1b**) has a barrier height of 111.6 kJ/mol, which means C4 hydrogen is easy to abstract compared to C1 hydrogen (Figure 3a). Then abstraction of C4 hydrogen leads to the formation of endothermic intermediate 3^{iPr}-**Int1b** with 24.3 kJ/mol energy. The transfer of C1 hydrogen to C4 carbon through the five-membered cyclic transition state 3^{iPr}-**TS2b** has an energy barrier of 23.9 kJ/mol with respect to 3^{iPr}-**Int1b**, to form **4′**. The lower energy pathway for the experimentally expected product (**4′**) is pathway **b** which has a barrier height of 111.6 kJ/mol (rate limiting step). Now, the experimentally observed dealkylated product (**4**) formation through pathway **c** has a barrier height of 46.4 kJ/mol. 3^{iPr}-**TS1c**) while the barrier height for pathway **d** is found to be 113.6 kJ/mol (3^{iPr}-**TS1d**) (Figure 3a). Among all the pathways explored for 3^{iPr}, the lower energy barrier is found to be for the C5 hydrogen abstraction which leads to the formation of **4**. This observation from the computational studies is in agreement with the experimental results. The formation of **4** is kinetically the preferred product for 3^{iPr} via transition state 3^{iPr}-**TS1c**.

Similarly, calculations have also been undertaken to understand the formation of **5** from the reaction of 3^{Me} with KHMDS (see Figure 3b). The transition state 3^{Me}-**TS1a** is found to have a barrier of 160.6 kJ/mol for pathway **a** while in pathway **b**, the first transition state 3^{Me}-**TS1b** has a barrier of only 29.5 kJ/mol energy. This clearly suggests that the C4 hydrogen abstraction takes place faster compared to C1 hydrogen. The abstraction of C4 hydrogen forms the intermediate 3^{Me}-**Int1b** which is slightly exothermic in nature with 8.0 kJ/mol energy. The 3^{Me}-**Int1b** yields **5** through the five-membered transition state 3^{Me}-**TS2b** and this has a barrier height of 55.5 kJ/mol energy with respect to 3^{Me}. The dealkylation pathway **c** to form **5′** is found to have a barrier height of 83.6 kJ/mol. Here, among all the pathways, the lower energy pathway is found to be pathway **b** which leads to the formation of **5** instead of the formation of **5′**. From the above mentioned observations, we can interpret that the formation of **5** takes place first via deprotonation at C4 followed by hydrogen abstraction from C1 by C4 via the five-membered transition state and not by the direct path as has been witnessed for species 3^{iPr}.

The triazaolefin, **5** is air and moisture sensitive although it is stable in an inert atmosphere. Even after heating the benzene-d_6 solution of **5** up to 80 °C for a prolonged period of time, we have not observed any kind of decomposition. Triazaolefin, **5** is a dense liquid at room temperature but could be crystallized at −20 °C as yellow color crystals. The molecular structure of **5** reveals that the central C1−C4 bond distance is 1.378(4) Å which indicates a double bond

Scheme 6. Schematic Representation of the Proposed Mechanism Including All the Possibilities for (a) 3^{iPr} and (b) 3^{Me}

(a)

(b)
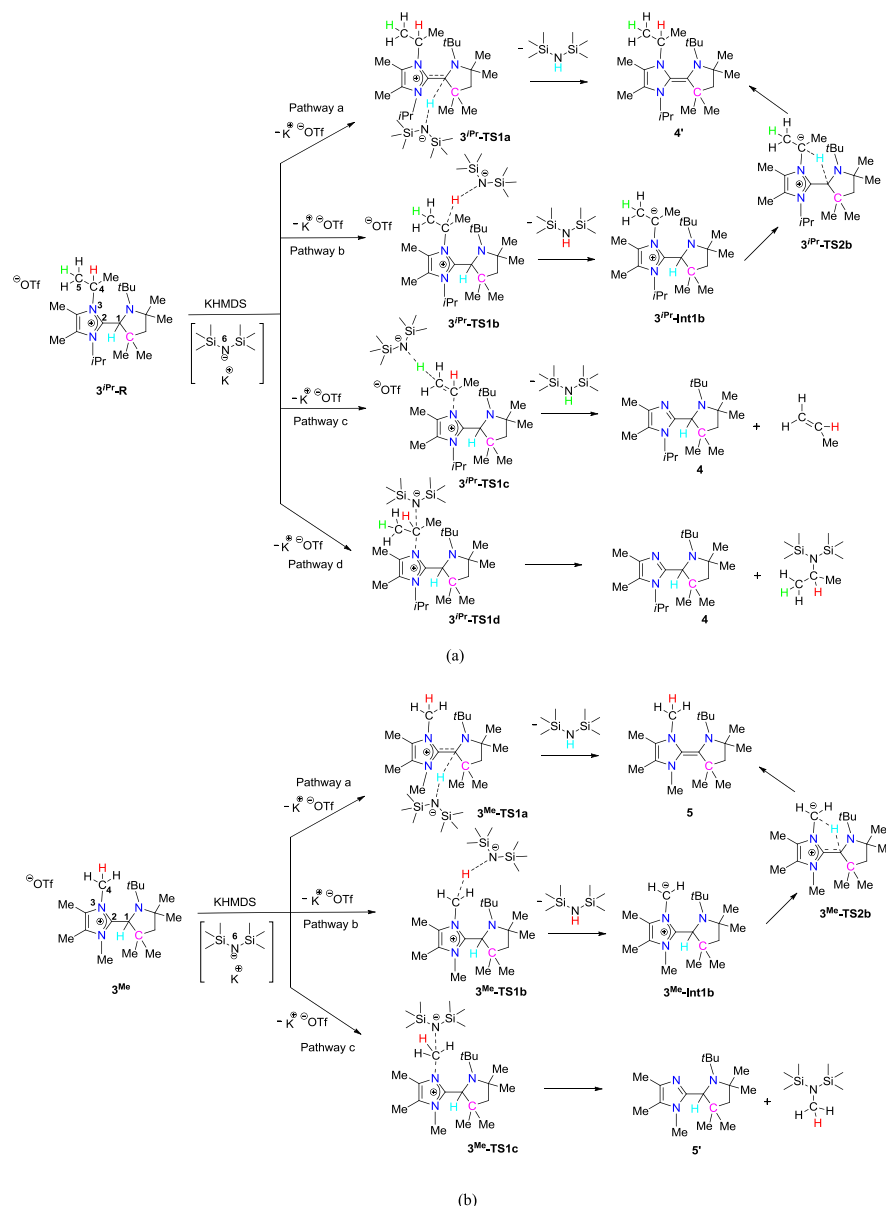
between them (Figure 2b). The molecular structure of **IV^{iPr}** is reported in the SI and it took about one month to obtained suitable single crystals for single-crystal XRD analysis from concentrated *n*-pentane solution at −20 °C (Scheme 2 and Figure S2 in Supporting Information). The C1−C4 bond length of **IV^{iPr}** is C1−C4 1.3583(18) Å which is very close to that of **5** (1.378(4) Å).

In the cyclic voltammogram (CV) of **5**, two reversible oxidation waves at half-wave potentials of 0.16 and 0.68 V (vs Ag wire as a pseudo reference, Figure 4) were observed.

Attempts at referencing the potentials against an internal standard were unsuccessful owing to reactions between the internal standards and the substrate molecules. The difference between the oxidation potentials is 0.52 V which is larger than that of TTF ($\Delta[E_{1/2}]$ = 0.37 V)[14] and translates to a comproportionation (K_c) value of 6.5 × 10^8 for the thermodynamic stability of the one-electron oxidized species. Despite this high K_c value, the redox stability of compound **5** (and accordingly of [**6**]) is poor as the responses in the CV

were seen to collapse on repeated cycling of the CV. This fact is likely an effect of the kinetic lability of the oxidized forms of **5** (see below). Apart from the aforementioned two oxidation steps, **5** also displays an irreversible reduction wave at −1.59 V (two small waves which are a follow-up of the oxidation waves are also observed).

Treatment of the triazaolefin, **5** with one equivalent of AgOTf initially produced an orange-red solution along with precipitation of metallic silver, but the orange-red color of the solution was discharged gradually. The ^{1}H NMR of the crude reaction mixture indicated the formation of diamagnetic compound, **3^{Me}**. The latter seems to form as a result of hydrogen abstraction from the solvent by the in situ-formed transient radical cation, **6** (Scheme 7).

The formation of **6** in solution has been confirmed by measuring the EPR spectrum of one-electron oxidized product of **5** with Ag$^+$. The X-band EPR spectrum displays a well-resolved signal centered at g = 2.003 (Figure 5). This spectrum was simulated by considering hyperfine coupling of
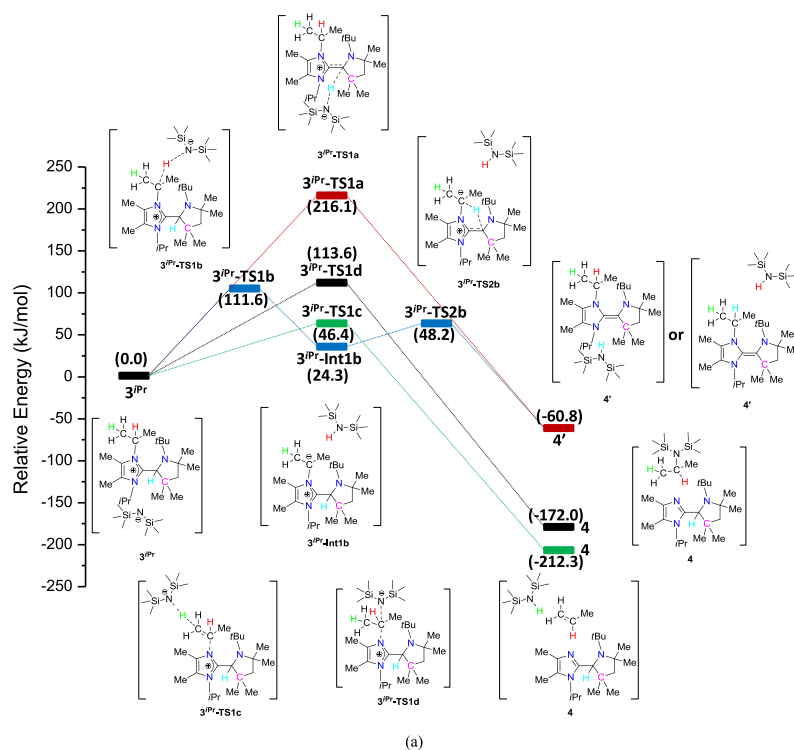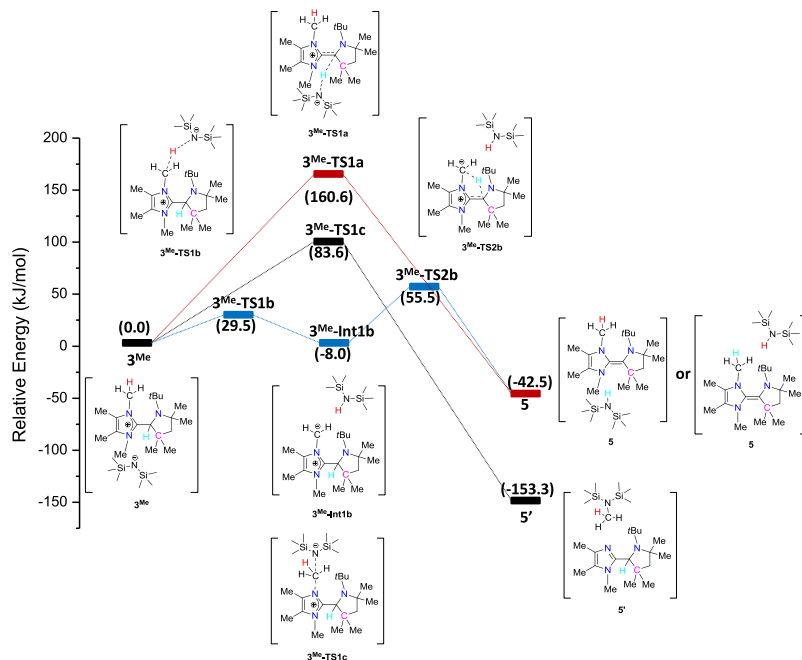
Figure 3. B3LYP-computed energy profile diagram for (a) 3^{iPr} and (b) 3^{Me}.

14.1, 11.6, and 9.9 MHz to three different ^{14}N nuclei. Calculations of the electron paramagnetic resonance (EPR) parameters at the TPSSh/EPR-III level of theory showed reasonable agreement between the simulated and the calculated values (Table S1). A Löwdin spin population analysis shows about 48% spin on the two carbon atoms of the alkene. Additionally, the spin on the N1 atom of the formally CAAC moiety is close to 25% (Figure S4, Table S2).[5a,c] While we were able to characterize the in-situ generated **6** through EPR spectroscopy, its stability was found

to be rather limited. Thus, the initially recorded EPR spectrum changed to a mixture of several other radical species within a span of 10 min at room temperature (Figures 6, S5 and S6). After 25 min, the signal converts to a predominant triplet. This fact is perhaps an indication for the generation of a species with a largely *N*-centered radical.

On the other hand, treatment of **5** with two equivalents of AgOTf resulted in the formation of **8** in an yield of about 80% (Scheme 7). The dication, **8** is most probably generated through isobutylene elimination[15] from the *N*-*t*Bu group of
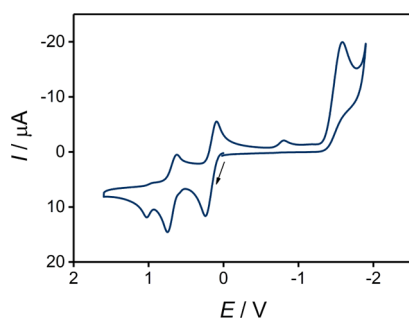
Figure 4. CV of **5** in THF/0.1 M NBu₄PF₆.

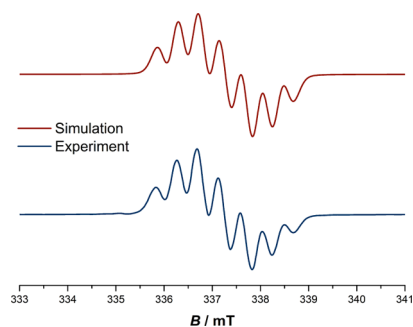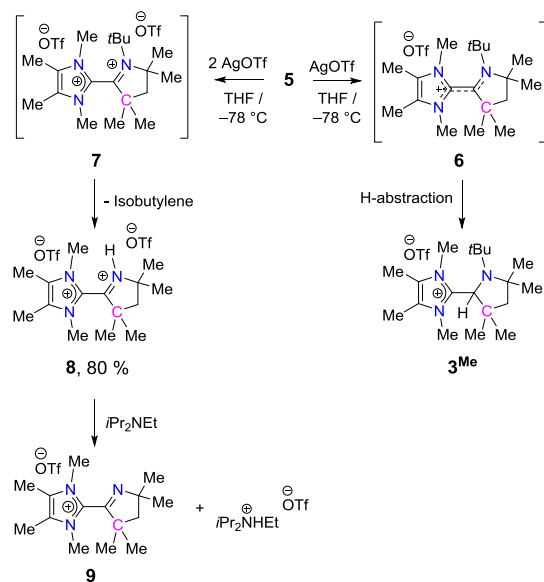**Scheme 7. 1:1 and 1:2 Reaction of 5 with AgOTf and Synthesis of 9**

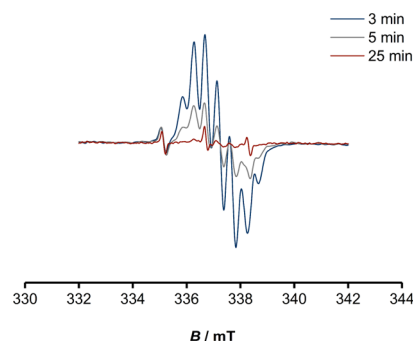**Figure 5.** Experimental (in THF at 295 K) and simulated EPR spectra of radical cation **6**.

Figure 6. Changes in the EPR spectrum of [**6**] over time. Measured in THF at 295 K.

The molecular structure of **8** (Figure 7a) reveals that the central C3−C8 distance is 1.482(5) Å which is closer to a C−C single bond.
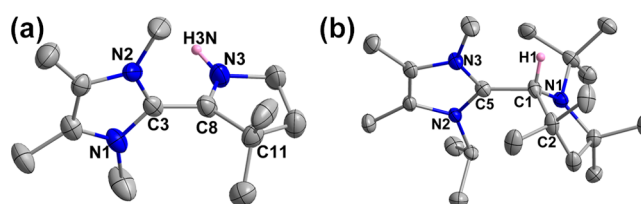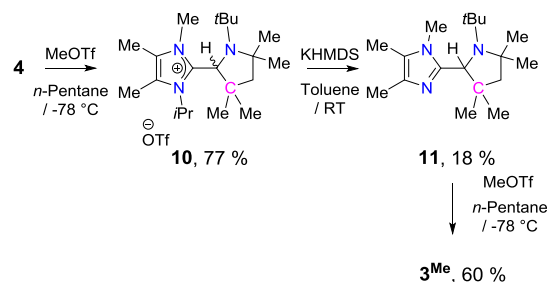

Figure 7. (a) Solid-state molecular structure of **8** (thermal ellipsoids at a 30% probability level; triflate anion and all H atoms except N3−H3N are omitted for clarity). Selected bond lengths (Å) and angles (°): N1−C3 1.327(4), N2−C3 1.324(5), N3−C8 1.273(5), C3−C8 1.482(5), N2−C3−N1 108.3(3), C3−C8−C11 127.4(3). (b) Solid-state molecular structure of **10** (thermal ellipsoids at a 30% probability level; the triflate anion and all H atoms except C1−H1 are omitted for clarity). Selected bond lengths (Å) and angles (°): N2−C5 1.346(3), N3−C5 1.342(3), N1−C1 1.472(3), C1−C5 1.527(3), N3−C5−N2 106.78(19), N1−C1−C2 106.79(19).

We also explored the possibility of using compound **4** as a synthon for the synthesis of a NHC−CAAC dimer. The reaction of **4** with MeOTf which leads to **10** (Scheme 8).
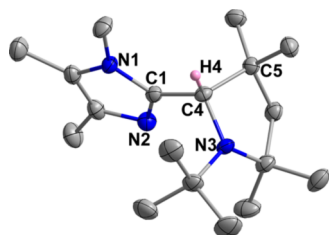
Scheme 8. Synthesis of 3^Me from 4

One of the isomeric forms of **10** could be crystallized and structurally characterized (Figure 7b).

Interestingly, when compound **10** was treated with KHMDS it underwent a dealkylation involving the *N-i*Pr group from the imidazolium moiety affording **11** (Scheme 8, Figure 8).

The central C1−C4 bond distance in **11** is 1.513(2) Å, indicating a single bond character. Finally, according to expectations, **11** could be converted to **3^Me** upon reaction with MeOTf (Scheme 8).

the pyrrolidinium moiety of the initially formed dication, **7**. Interestingly, the isolation of the corresponding radical cation and dication was possible containing *N-i*Pr unit in the formal CAAC part, which underscores the importance of *N*-substitution in tuning the reactivity of these species.[5c] Subsequently, we have tried to deprotonate the dication, **8** using *i*Pr₂NEt resulting in the formation of the anticipated monocation, **9** along with *i*Pr₂NEtHOTf. Because of the similar solubility of both compounds we were unable to isolate pure **9**.

Figure 8. Solid-state molecular structure of **11** (thermal ellipsoids at 30% and all H atoms except C4–H4 are omitted for clarity). Selected bond lengths (Å) and angles (°): N1–C1 1.372(2), N2–C1 1.321(2), N3–C4 1.464(2), C1–C4 1.513(2), N2–C1–N1 110.74(15), N3–C4–C5 102.47(13).

3. CONCLUSIONS

In summary, we reveal effects of N-substitution (N-iPr vs N-tBu) of the CAAC scaffold on the formation and oxidation of NHC–CAAC derived triazaalkenes. While N-iPr substitution on the imidazolium scaffold leads to the N–C bond cleavage, N–Me substitution leads to the formation of triazaalkene. The reactivity of these two entities has also been demonstrated. DFT studies have been undertaken to understand the mechanistic insights into the dealkylation (3^{iPr}) versus deprotonation (3^{Me}) with KHMDS. This reveals that the dealkylation of 3^{iPr} via 3^{iPr}-**TS1b** has the lowest barrier of 46.4 kJ/mol while other pathways are estimated to be higher in energy (216.1 kJ/mol for 3^{iPr}-**TS1a**, 111.6 kJ/mol for 3^{iPr}-**TS1b** and 113.6 kJ/mol for 3^{iPr}-**TS1d**). On the other hand, for 3^{Me} the barrier height for deprotonation from C4 position is estimated to be the lowest (29.5 kJ/mol for 3^{Me}-**TS1b**) compared to 3^{Me}-**TS1a** (160.6 kJ/mol) and 3^{Me}-**TS2c** (83.6 kJ/mol). This clearly suggests that a small substitution drastically alters the mechanistic pathway and hence alkyl substitution at the N-position is critical in deciding product selectivity.

4. EXPERIMENTAL SECTION

All experiments were carried out under an argon atmosphere using standard Schlenk techniques or in a PL-HE-2GB Innovative Technology GloveBox and MBraun Unilab SP GloveBox. n-Hexane, diethyl ether, THF, and toluene were dried by the PS-MD-5 Innovative Technology solvent purification system. tert-Butyl amine (98%) was purchased from Alfa Aesar. Diisopropylamine (98%), isobutyraldehyde (97%) were purchased from AVRA. Isobutylene oxide (97%) and triflic anhydride (98%) were purchased from TCI chemicals. KHMDS (95%) and silver triflate (99%) were purchased from Sigma-Aldrich. All chemicals except diisopropylamine were used without further purifications. Diisopropylamine was distilled over NaOH under argon. 1^{Me},[16] 1^{iPr},[16] and **2**,[17] were prepared according to literature procedures. Benzene-d_6 was dried and distilled over potassium under argon. Chloroform-d_1 and acetonitrile-d_3 were dried and distilled over CaH₂ under argon. UV/vis spectra were acquired using Jasco V-670 spectrometer using quartz cells with a path length of 0.1 cm. NMR spectra were recorded on a BrukerNanoBay 300 MHz NMR spectrometer. ¹H and ¹³C{¹H} NMR spectra were referenced to the peaks of residual protons of the deuterated solvent (¹H) or the deuterated solvent itself (¹³C{¹H}). ¹⁹F{¹H} NMR spectra were referenced to external toluene−CF₃. We have used ¹H–¹H COSY, ¹H–¹³C{¹H} HMQC and ¹H–¹³C{¹H} HMBC to confirm the NMR peaks assignments. Mass spectrometry was performed on an Agilent 6210 ESI-TOF in positive mode, using high-performance liquid chromatography grade solvents. In case of 3^{Me}, 3^{iPr}, **4**, **5**, **8**, **10**, and **11** elemental analyses were performed on a VARIO EL. Melting points were determined in closed NMR tubes under argon atmosphere and are uncorrected.

4.1. Synthesis of 2^{tBu}. (a) Anhydrous sodium sulfate (20 g) was added to the DCM solution of isobutyraldehyde (24.95 g, 34.5 mmol, in 100 mL of DCM). Then tert-butylamine (25.23 g, 34.5 mmol) was added slowly on it at 0 °C and the mixture was stirred overnight at room temperature. The resulting solution was filtered and after fractional distillation, the desired imine was obtained as a colorless liquid. Yield: 30.4 g, 23.89 mmol (69.2%). ¹H NMR (300 MHz, CDCl₃, 298 K): δ 0.99 (d, ³J_{HH} = 6.88 Hz, 6H, CH(CH₃)₂), 1.11 (s, 9H, C(CH₃)₃), 2.27−2.43 (m, 1H, CH(CH₃)₂), 7.34 (d, ³J_{HH} = 6.04 Hz, 1H, N═CH) ppm. (b) The resulting imine (11 mL, 66.52 mmol) was dissolved in dry diethyl ether (100 mL) in a 500 mL Schlenk flask. Then LDA (70 mL, 70 mmol, 1 M solution in THF and hexane) was added dropwise to it at 0 °C. Ice bath was removed after complete addition of LDA and the reaction mixture was stirred for another 3 h at room temperature. Subsequently, all the volatiles were removed under vacuum and the resulting residue was dissolved in diethyl ether (250 mL) and then, isobutylene oxide (6.70 mL, 73.18 mmol) was added slowly at room temperature. The reaction mixture was stirred for 12 h. After that, trifluoromethane sulfonic anhydride (13 mL, 75.72 mmol) was added at −78 °C. An immediate white precipitation was formed. The reaction mixture was allowed to reach room temperature slowly and stirred for another 1 h at room temperature. After that, the resulting solution was filtered and the residue was washed with diethyl ether (50 mL) followed by ethyl acetate (30 mL). Drying of resulting white powder under vacuum gave target compound **2**. Single crystals suitable for X-ray diffraction were obtained by layering of petroleum ether on saturated DCM solution at room temperature after 2 days. Yield: 9.67 g, 29.17 mmol (43.87%). mp: 156 °C (decomposed). ¹H NMR (300 MHz, CDCl₃, 298 K): δ 1.46 (s, 6H, C(CH₃)₂), 1.71 (s, 9H, C(CH₃)₃), 1.77 (s, 6H, NC(CH₃)₂), 2.16 (s, 2H, CH₂), 9.08 (s, 1H, CH) ppm. ¹³C{¹H} NMR (75.43 MHz, CDCl₃, 298 K): δ 26.1 (C(CH₃)₂), 30.5 (C(CH₃)₃), 31.0 (C(CH₃)₂), 45.3 (C(CH₃)₂), 52.9 (CH₂), 68.0 (C(CH₃)₃), 82.3 (C(CH₃)₂), 120.9 (q, ¹J_{CF} = 320 Hz, CF₃SO₃⁻), 187.1 (CH) ppm. ¹⁹F{¹H} NMR (169.2 MHz, CDCl₃, 298 K): δ −78.3 ppm.

4.2. Synthesis of 3^{Me}. Dry THF (30 mL) was added to the mixture of 1^{Me} (1 g, 8.052 mmol) and **2** (2.54 g, 7.664 mmol) at room temperature. Then the reaction mixture was stirred for 17 h at room temperature. On evaporation of all the volatiles followed by washing with n-hexane (50 mL), a white solid was obtained as desired product 3^{Me}. Single crystals suitable for X-ray diffraction were obtained by slow diffusion of n-pentane into a saturated THF solution of 3^{Me} at room temperature after 2 days. Yield: 3.290 g, 7.22 mmol (94%). mp: 96−98 °C. ¹H NMR (300 MHz, CDCl₃, 298 K): δ 0.67 (s, 3H, NC(CH₃)₂), 1.06 (s, 9H, C(CH₃)₃), 1.44 (s, 3H, NC(CH₃)₂), 1.47 (s, 6H, C(CH₃)₂), 1.78 (d, 1H, CH₂), 2.03 (d, 1H, CH₂), 2.25 (s, 3H, NC(CH₃)), 2.29 (s, 3H, NC(CH₃)), 3.74 (s, 3H, NCH₃), 4.07 (s, 3H, NCH₃), 4.58 (s, 1H, CH) ppm. ¹³C{¹H} NMR (75.43 MHz, CDCl₃, 298 K): δ 8.8 (NC(CH₃)), 9.1 (NC(CH₃)), 27.8 (NC(CH₃)₂), 29.5 (C(CH₃)₃), 29.6 (C(CH₃)₂), 32.2 (C(CH₃)₂), 32.5 (NCH₃), 32.9 (NCH₃), 33.1 (NC(CH₃)₂), 41.5 (C(CH₃)₂), 55.7 (C(CH₃)₃), 59.3 (CH₂), 64.5 (NC(CH₃)₂), 67.6 (CH), 121.0 (q, ¹J_{CF} = 320 Hz, CF₃SO₃⁻), 126.6 (NCCN), 126.7 (NCCN), 147.4 (NCN) ppm. ¹⁹F{¹H} NMR (169.2 MHz, CDCl₃, 298 K): δ −78.2 ppm. HRMS (ESI-TOF) m/z: [M]⁺ Calcd for [C₁₉H₃₆N₃]⁺, 306.2904; found 306.2904. Anal. Calcd for C₂₀H₃₆F₃N₃O₃S (455.24): C, 52.73; H, 7.97; N, 9.22; S, 7.04. Found: C, 52.78; H, 7.99; N, 9.28; S 7.06.

4.3. Synthesis of 3^{iPr}. Dry THF (30 mL) was added to the mixture of 1^{iPr} (1.510 g, 8.375 mmol) and **2** (2.636 g, 7.954 mmol). Then the reaction mixture was stirred for 17 h at room temperature. On evaporation of all the volatiles followed by washing with n-hexane (2 × 25 mL), a white solid was obtained as the desired product 3^{iPr}. Single crystals suitable for X-ray diffraction were obtained by slow diffusion of n-pentane into a saturated THF solution of 3^{iPr} at room temperature after 2 days. Yield: 3. 658 g, 7.149 mmol (90%). mp: 172−174 °C. ¹H NMR (300 MHz, CDCl₃, 298 K): δ 0.77 (s, 3H, CH₃), 1.12 (s, 9H, C(CH₃)₃), 1.38 (s, 3H, CH₃), 1.50 (s, 3H, CH₃), 1.53 (s, 3H, CH₃), 1.61 (d, 3H,

NCH(CH_3)$_2$), 1.63 (d, 3H, NCH(CH_3)$_2$), 1.65 (d, 3H, NCH-(CH_3)$_2$), 1.71 (d, 3H, NCH(CH_3)$_2$), 1.83 (d, 1H, CH_2), 2.01 (d, 1H, CH_2), 2.41 (s, 3H, NCCH_3), 2.42 (s, 3H, NCCH_3), 4.72 (s, 1H, NCH), 4.80 (sep, 1H, NCH(CH$_3$)$_2$), 6.13 (sep, 1H, NCH(CH$_3$)$_2$) ppm. ^{13}C{^{1}H} NMR (75.43 MHz, CDCl$_3$, 298 K): δ 11.0 (N$_{NHC}$CCH_3), 11.3 (N$_{NHC}$CCH_3), 20.8 (NCH(CH_3)$_2$), 21.0 (NCH(CH_3)$_2$), 21.6 (NCH(CH_3)$_2$), 21.8 (NCH(CH_3)$_2$), 28.0 (N$_{CAAC}$CCH_3), 29.8 (NC(CH_3)$_3$), 30.3 (N$_{CAAC}$CCH_3), 31.9 (HCCCH_3), 32.9 (HCCCH_3), 40.9 (HCCCH_3), 48.4 (NC(CH$_3$)$_2$), 50.8 (NC(CH$_3$)$_2$), 56.0 (NC(CH$_3$)$_3$), 58.4 (CH_2), 64.4 (N$_{CAAC}$$C$(C$H_3$)$_2$), 68.8 (N$C$H), 121.1 (q, $^1J_{CF}$ = 320 Hz, CF_3SO$_3$$^-$), 127.6 (N$_{NHC}$$CCH_3$), 127.7 (N$_{NHC}$$CCH_3$), 147.1 (N$C$N) ppm. ^{19}F{^{1}H} NMR (169.2 MHz, CDCl$_3$, 298 K): δ −78.1 ppm. HRMS (ESI-TOF) m/z: [M]$^+$ Calcd for [C$_{23}$H$_{44}$N$_3$]$^+$, 362.3530; found: 362.3530. Anal. Calcd for C$_{24}$H$_{44}$F$_3$N$_3$O$_3$S (511.31): C, 56.34; H, 8.67; N, 8.21; S, 6.27. Found: C, 56.44; H, 8.70; N, 8.28; S, 6.35.

4.4. Synthesis of 4. Dry toluene (40 mL) was added to the mixture of 3^{iPr} (0.803 g, 1.569 mmol) and KHMDS (0.329 g, 1.569 mmol) at room temperature. Then the reaction mixture was stirred for 4 h. Subsequently, the reaction mixture was filtered and on evaporation of the filtrate under vacuum, a light yellow colored dense liquid of 4 was obtained. Single crystals suitable for X-ray diffraction were obtained from saturated n-pentane solution at −35 °C after 15 days. Yield: 0.260 g, 0.813 mmol (51%). mp: 67−69 °C. ^{1}H NMR (300 MHz, C$_6$D$_6$, 298 K): δ 0.68 (s, 3H, CC(CH_3)$_2$), 1.11 (dd, 6H, NCH(CH_3)$_2$), 1.21 (s, 9H, C(CH_3)$_3$), 1.40 (s, 3H, CC(CH_3)$_2$), 1.47 (d, 2H, CH_2), 1.57 (s, 3H, NC(CH_3)$_2$), 1.96 (s, 3H, NCCH_3), 2.06 (s, 3H, NC(CH_3)$_2$), 2.25 (s, 3H, NCCH_3), 2.93 (d, 1H, CH_2), 4.15 (s, 1H, CH), 4.25 (sep, 1H, CH(CH$_3$)$_2$) ppm. ^{13}C{^{1}H} NMR (75.43 MHz, CDCl$_3$, 298 K): δ 11.4 (N$_{NHC}$CCH_3), 13.4 (N$_{NHC}$CCH_3), 22.1 (CH(CH_3)$_2$), 25.7 (CC(CH_3)$_2$), 30.7 (CC(CH_3)$_2$), 31.8 (C(CH_3)$_3$), 32.6 (NC(CH_3)$_2$), 33.5 (NC(CH_3)$_2$), 40.2 (CC(CH$_3$)$_2$), 46.3 (CH(CH$_3$)$_2$), 53.8 (C(CH_3)$_2$), 56.7 (CH_2), 61.8 (NC(CH$_3$)$_2$), 66.5 (N$_{CAAC}$CHC), 119.7 (NCCH_3), 134.0 (NCCH$_3$), 149.5 (NCN) ppm. HRMS (ESI-TOF) m/z: [M + H]$^+$ Calcd for [C$_{19}$H$_{35}$N$_3$ + H]$^+$, 320.3060; found: 320.3079. Anal. Calcd for C$_{20}$H$_{37}$N$_3$ (319.30): C, 75.18; H, 11.67; N, 13.15. Found: C, 75.18; H, 11.70; N, 13.27.

4.5. Synthesis of 5. Dry toluene (75 mL) was added to the mixture of 3^{Me} (4.04 g, 8.867 mmol) and KHMDS (1.862 g, 8.867 mmol) at room temperature. Then the reaction mixture was stirred for 4 h. The solution was filtered and after removal of the filtrate under vacuum, a bright yellow colored dense liquid was obtained as the desired product 5. On keeping the triazaolefin, 5 at −20 °C for 2 months bright yellow color crystals of olefin 5 suitable for X-ray diffraction were obtained. Yield: 2.48 g, 8.117 mmol (91%). mp: 51−53 °C. ^{1}H NMR (300 MHz, C$_6$D$_6$, 298 K): δ 1.34 (s, 3H, CCH_3), 1.39 (s, 9H, C(CH_3)$_3$), 1.43 (s, 3H, CCH_3), 1.52 (s, 6H, N$_{NHC}$CCH_3), 1.57 (s, 3H, CCH_3), 1.58 (d, 1H, CH_2), 1.64 (s, 3H, CCH_3), 1.85 (d, 1H, CH_2), 2.83 (s, 3H, N$_{NHC}$CCH_3), 3.27 (s, 3H, N$_{NHC}$CH_3) ppm. ^{13}C{^{1}H} NMR (75.43 MHz, C$_6$D$_6$, 298 K): δ 9.4 (CCH_3), 10.2 (CCH_3), 28.8 (NCH_3), 30.8 (NCH_3), 31.0 (CCH_3), 31.6 (C(CH_3)$_3$), 33.6 (CCH_3), 41.4 (C(CH_3)$_2$), 42.7 (NCH_3), 58.1 (C(CH$_3$)$_3$), 61.8 (CH_2), 61.8 (C(CH_3)$_2$), 102.9 (N$_{CAAC}$CC), 118.2 (N$_{NHC}$CCH_3), 120.3 (N$_{NHC}$CCH_3), 151.0 (NCN) ppm. UV/vis (n-hexane): λ_{max} (ε) = 300 (8132.9) nm (Lmol^{-1} cm^{-1}). HRMS (ESI-TOF) m/z: [M + H]$^+$ Calcd for [C$_{19}$H$_{35}$N$_3$ + H]$^+$, 306.2904; found: 306.2930. Anal. Calcd for C$_{17}$H$_{27}$F$_6$N$_3$O$_6$S$_2$ (305.51): C, 74.70; H, 11.55; N, 13.75. Found: C, 74.68; H, 31.94; N, 13.55 (due to the sensitivity of the compound we were not able to get satisfactory elemental analysis data).

4.6. Reaction of 5 with 1 equiv AgOTf. Inside the glovebox at room temperature, AgOTf solution (0.175 g, 0.681 mmol in about 8 mL THF) was added dropwise to triazaolefin 5 solution (0.209 g, 0.684 mmol in 10 mL THF) at −78 °C with continuous stirring. After complete addition of AgOTf solution, the reaction mixture was stirred for 3 h. On evaporating all the volatiles, the obtained solid was extracted with n-hexane. The n-hexane extract was evaporated and ^{1}H NMR was recorded in C$_6$D$_6$ which did not show any peak

of unreacted triazaolefin, 5. Then ^{1}H NMR of the residue was taken in CD$_3$CN and compared with the ^{1}H NMR of compound 3^{Me} in CD$_3$CN which confirmed the formation of 3^{Me}.

4.7. Synthesis of 8. AgOTf solution (0.694 g, 2.703 mmol, 10 mL THF) was added to the solution of 5 (0.413 g, 1.351 mmol, 15 mL THF) at −78 °C. Then the reaction mixture was slowly allowed to reach room temperature over a period of 3 h and then stirred for further 2 h at room temperature. Subsequently, all volatiles were evaporated and the residue was extracted with dry acetonitrile (15 mL). After evaporation of the filtrate, an off-white solid compound was obtained as desired product 8. Single crystals suitable for X-ray diffraction were obtained by slow diffusion of diethylether into a saturated acetonitrile solution of 8 at room temperature after 3 days. Yield: 0.594 g, 1.084 mmol (80.3%). mp: 182−184 °C. ^{1}H NMR (300 MHz, CD$_3$CN, 298 K): δ 1.55 (s, 6H, C(CH_3)$_2$), 1.73 (s, 6H, C(CH_3)$_2$), 2.32 (s, 6H, NCCH_3), 2.41 (s, 2H, CH_2), 3.69 (s, 6H, NCH_3) ppm. ^{13}C{^{1}H} NMR (75.43 MHz, CD$_3$CN, 298 K): δ 9.0 (NCCH_3), 27.1 (C(CH_3)$_2$), 28.6 (C(CH_3)$_2$), 35.8 (NCH_3), 48.9 (CH_2), 56.7 (C(CH$_3$)$_2$), 75.9 (C(CH$_3$)$_2$), 121.6 (q, $^1J_{CF}$ = 320 Hz, CF_3SO$_3$$^-$), 133.2 (N$CCH_3$) ppm. ^{19}F{^{1}H} NMR (169.2 MHz, CD$_3$CN, 298 K): δ −78.5 ppm. HRMS (ESI-TOF) m/z: [M − H]$^+$ Calcd for [C$_{15}$H$_{27}$N$_3$−H]$^+$, 248.2121; found: 248.2128. Anal. Calcd for C$_{17}$H$_{27}$F$_6$N$_3$O$_6$S$_2$ (547.12): C, 37.29; H, 4.97; N, 7.67; S, 11.71. Found: C, 37.39; H, 5.03; N, 7.77; S, 11.75.

4.8. Synthesis of 9. iPr$_2$NEt (0.044 mL) was added to a suspension of 8 (0.131 g, 0.239 mmol, 15 mL THF) at −78 °C. Then the reaction mixture was allowed to reach room temperature and stirred for another 2 h at room temperature. During this, the suspension got completely dissolved and a clear brownish solution was formed. On evaporation of all the volatiles, a pale brown-colored solid was obtained which is a 1:1 mixture of 9 and iPr$_2$NEtHOTf. We were not able to get pure compound of 9 even after repeating crystallization and which always contained iPr$_2$NEtHOTf. Therefore, we only reported the ^{1}H and ^{19}F{^{1}H} NMR data from the 1:1 mixture of 9 and iPr$_2$NEtHOTf. ^{1}H NMR (300 MHz, CD$_3$CN, 298 K): δ 1.26 (s, 6H, C(CH_3)$_2$), 1.32 (d, 12H, CH(CH_3)$_2$), 1.33 (t, 3H, CH$_2$CH_3), 1.40 (s, 6H, C(CH_3)$_2$), 1.98 (s, 2H, CH_2), 2.24 (s, 6H, CCH_3) 3.15 (q, 2H, CH_2CH$_3$), 3.58 (s, 6H, NCH_3), 3.65 (sep, 2H, CH(CH$_3$)$_2$) ppm. ^{19}F{^{1}H} NMR (169.2 MHz, CD$_3$CN, 298 K): δ −79.3 ppm.

4.9. Synthesis of 10. A solution of 4 (0.589 g, 1.843 mmol, 10 mL n-pentane) was added to a MeOTf solution (0.303 g, 1.846 mmol, in 5 mL n-pentane) at −78 °C and allowed to reach room temperature in 1 h. Then the mixture was stirred for 3 h at room temperature which resulted in a colorless turbid solution. On evaporation of all volatiles, white solids of 10 were obtained as an isomeric mixture of products. Single crystals suitable for X-ray diffraction were obtained by slow diffusion of n-pentane into a saturated THF solution of compound 10 at −35 °C after 5 days. Yield: 0.690 g, 1.426 mmol (77%). mp: 137−139 °C. ^{1}H NMR (300 MHz, CD$_3$CN, 298 K): δ 0.65 (s, 3H, C(CH_3)$_2$), 0.68 (s, 3H, C(CH_3)$_2$), 1.07 (s, 9H, C(CH_3)$_3$), 1.11 (s, 9H, C(CH_3)$_3$), 1.39 (s, 3H, C(CH_3)$_2$), 1.45 (s, 6H, C(CH_3)$_2$), 1.47 (s, 6H, C(CH_3)$_2$), 1.53 (s, 3H, C(CH_3)$_2$), 1.54−1.62 (m, 12H, CH(CH_3)$_2$), 1.83 (m, 2H, CH_2), 2.02 (m, 2H, CH_2), 2.15 (q, 3H, CCH_3), 2.16 (q, 3H, CCH_3), 2.35 (s, 6H, CCH_3), 3.61 (s, 3H, NCH_3), 4.03 (s, 3H, NCH_3), 4.59 (s, 1H, NCHC), 4.73 (s, 1H, NCHC), 4.88 (sep, 1H, CH(CH$_3$)$_2$), 6.10 (sep, 1H, CH(CH$_3$)$_2$) ppm. ^{13}C{^{1}H} NMR (75.43 MHz, CD$_3$CN, 298 K): δ 8.6 (1C, CCH_3), 8.9 (1C, CCH_3), 11.1 (1C, CCH_3), 11.3 (1C, CCH_3), 20.8 (1C, CH(CH_3)$_2$), 21.2 (1C, CH(CH_3)$_2$), 21.4 (1C, CH(CH_3)$_2$), 21.6 (1C, CH(CH_3)$_2$), 27.3 (1C, C(CH_3)$_2$), 28.3 (1C, C(CH_3)$_2$), 29.5 (1C, C(CH_3)$_2$), 29.6 (3C, C(CH_3)$_3$), 29.9 (3C, C(CH_3)$_3$), 30.5 (1C, C(CH_3)$_2$), 31.9 (1C, C(CH_3)$_2$), 32.3 (1C, C(CH_3)$_2$), 33.1 (1C, C(CH_3)$_2$;1C, NCH_3), 33.2 (1C, C(CH_3)$_2$), 34.1 (1C, NCH_3), 41.8 (2C, C(CH_3)$_2$), 56.4 (1C, C(CH$_3$)$_3$), 56.5 (1C, C(CH$_3$)$_3$), 122.1 (q, $^1J_{CF}$ = 320 Hz, CF_3SO$_3$$^-$), 126.1 (1C, NCC$H_3$), 126.5 (1C, NCC$H_3$), 148.0 (1C, N$C$N), 58.6 (1C, C$H_2$), 59.7 (1C, C$H_2$), 65.0 (1C, C(CH$_3$)$_2$), 65.1 (1C, C(CH$_3$)$_2$), 67.5 (1C, NCHC), 69.6 (1C, NCHC), 129.3 (1C, CH$_3$NCCH_3), 129.8 (1C, CH$_3$NCCH_3), 147.5

(1C, NCN), 148.0 (1C, NCN) ppm. ^{19}F{^{1}H} NMR (169.2 MHz, CD$_3$CN, 298 K): δ −79.3 ppm. HRMS (ESI-TOF) m/z: [M]$^+$ Calcd for [C$_{21}$H$_{40}$N$_3$]$^+$, 334.3217; found: 334.3217. Anal. Calcd for C$_{22}$H$_{40}$F$_3$N$_3$O$_3$S (483.27): C, 54.64; H, 8.34; N, 8.69; S, 6.63. Found: C, 54.88; H, 8.36; N, 8.72; S, 6.73.

4.10. Synthesis of 11. Dry toluene (100 mL) was added to the isomeric mixture of **10** (2.632 g, 5.442 mmol) and KHMDS (1.142 g, 5.442 mmol) at room temperature. Then the reaction mixture was stirred for 4 h. The solution was filtered and after removal of the filtrate under vacuum, a deep brown-colored dense liquid was obtained. Single crystals of **11**, suitable for X-ray diffraction were obtained from saturated *n*-pentane solution at −35 °C after 20 days. Yield: 0.220 g, 1.00 mmol (18%). mp: 71−73 °C. ^{1}H NMR (300 MHz, C$_6$D$_6$, 298 K): δ 0.59 (s, 3H, HCC(CH_3)$_2$), 1.19 (s, 9H, C(CH_3)$_3$), 1.37 (s, 3H, HCC(CH_3)$_2$), 1.55 (s, 3H, NC(CH_3)$_2$), 1.71 (s, 3H, MeNCCH_3), 2.03 (s, 3H, NC(CH_3)$_2$), 2.26 (s, 3H, NCCH_3), 2.81 (s, 3H, NCH_3), 3.99 (s, 1H, CH), (*resonances for CH$_2$-moiety of pyrrolidinyl scaffold were not found at room temperature*) ppm. ^{13}C{^{1}H} NMR (75.43 MHz, C$_6$D$_6$, 298 K): δ 8.9 (MeNCCH_3) 13.5 (NCCH_3), 25.0 (1C, CHC(CH_3)$_2$), 29.5 (NCH_3), 30.6 (1C, CHC(CH_3)$_2$), 31.7 (C(CH_3)$_3$), 33.0 (1C, NC(CH_3)$_2$), 33.1 (1C, NC(CH_3)$_2$), 40.3 (CHCMe$_2$), 53.8 (CMe_3), 56.7 (CH_2), 61.8 (NC(CH$_3$)$_2$), 66.7 (NCHCMe2), 120.5 (MeNCMeCMe), 132.0 (NCMeCMe), 149.9 (CN) ppm. HRMS (ESI-TOF) m/z: [M + H]$^+$ Calcd for [C$_{18}$H$_{33}$N$_3$ + H]$^+$, 292.2747; found: 292.2746. Anal. Calcd for C$_{18}$H$_{33}$N$_3$ (291.48): C, 74.17; H, 11.41; N, 14.42. Found: C, 74.42; H, 11.59; N, 14.56.

4.11. Reaction of 11 with MeOTf (Formation of 3^{Me}). A solution of MeOTf (0.1644 g, 1.00 mmol, 30 mL *n*-pentane) was added to the *n*-pentane solution of **11** (0.220 g, 1.00 mmol, in 20 mL of *n*-pentane) at −78 °C and allowed to reach room temperature in 3 h in stirring conditions. Then the mixture was stirred for 2 h at room temperature which resulted in a white turbid solution. On filtration through D-4 frit, white solids were obtained. The ^{1}H NMR spectrum of the white solid exactly matches with previously obtained 3^{Me} compound. Yield: 0.2754 g, 0.604 mmol (60%).

4.12. Theoretical Calculations. DFT calculations for mechanistic studies were carried out using Gaussian 09 suite of program.[18] The geometry optimizations were performed at the B3LYP/6-31G* level of theory.[19] Frequency calculations have also been performed at the same level of theory to check the stationary points (zero negative frequency) and first order saddle point (single negative frequency) for the transition state. Using the optimized geometries, further single-point calculations have been performed employing TZVP basis set for all atoms. The solvent effect was incorporated using polarizable continuum model (PCM) with THF as a solvent.[20] All the energies reported here are Gibbs free energies.

All calculations related to the computation of EPR parameters were performed on the Soroban cluster of the High-Performance Computing Center of the Freie Universität Berlin using the ORCA 4.0.1 program suite.[21] In all calculations, solvent effects were modeled using the conductor-like PCM (CPCM)[22] with THF as solvent while dispersion was accounted for by employing Grimme's D3 correction with Becke−Johnson damping.[23] Convergence criteria were set tight for both optimizations (TIGHTOPT) and SCF calculations (TIGHTSCF). Restricted and unrestricted DFT methods were employed for closed- and open-shell species, respectively. Geometries of the native and singly oxidized species were optimized using the BP86 functional[24] and the def2-TZVP basis set. The absence of imaginary frequencies in numerical frequency calculations verified that true minima were obtained. For geometry optimizations and numerical frequency calculations, the resolution of identity approximation[25] with corresponding auxiliary basis sets[26] was used to save computational costs. Single-point calculations and calculations of EPR parameters of the singly oxidized species were performed using the TPSSh[27] functional and the EPR-III basis set.[28] Spin densities were calculated according to the Löwdin spin population and visualized using the modified Avogadro 1.2.0 program with an extended ORCA support.[29]

ASSOCIATED CONTENT

Ⓢ Supporting Information

The Supporting Information is available free of charge on the ACS Publications website at DOI: 10.1021/acs.joc.9b00774.

Plots of NMR spectra for new compounds, UV/vis spectra, and complete details of computational calculations (PDF)

Crystallographic details and data (CIF)

AUTHOR INFORMATION

Corresponding Authors
*E-mail: rajaraman@chem.iitb.ac.in (G.R.).
*E-mail: carola.schulzke@uni-greifswald.de (C.S.).
*E-mail: biprajit.sarkar@fu-berlin.de (B.S.).
*E-mail: vc@tifrh.res.in (V.C.).
*E-mail: ajana@tifrh.res.in (A.J.).

ORCID ⊙
Pankaj Kalita: 0000-0002-1240-5633
Gopalan Rajaraman: 0000-0001-6133-3026
Biprajit Sarkar: 0000-0003-4887-7277
Vadapalli Chandrasekhar: 0000-0003-1968-2980
Anukul Jana: 0000-0002-1657-1321

Notes
The authors declare no competing financial interest.

REFERENCES

(1) (a) Melaimi, M.; Jazzar, R.; Soleilhavoup, M.; Bertrand, G. Cyclic (Alkyl)(amino)carbenes (CAACs): Recent Developments. *Angew.Chem. Int. Ed.* **2017**, *56*, 10046−10068. (b) Soleilhavoup, M.; Bertrand, G. Cyclic (Alkyl)(Amino)Carbenes (CAACs): Stable Carbenes on the Rise. *Acc. Chem. Res.* **2015**, *48*, 256−266.

(2) Turner, Z. R. Chemically Non-Innocent Cyclic (Alkyl)-(Amino)Carbenes: Ligand Rearrangement, C−H and C−F Bond Activation. *Chem.—Eur. J.* **2016**, *22*, 11461−11468.

(3) (a) Martin, D.; Canac, Y.; Lavallo, V.; Bertrand, G. Comparative Reactivity of Different Types of Stable Cyclic and Acyclic Mono- and Diamino Carbenes with Simple Organic Substrates. *J. Am. Chem. Soc.* **2014**, *136*, 5023−5030. (b) Lavallo, V.; Canac, Y.; Donnadieu, B.; Schoeller, W. W.; Bertrand, G. CO Fixation to Stable Acyclic and Cyclic Alkyl Amino Carbenes: Stable Amino Ketenes with a Small HOMO−LUMO Gap. *Angew. Chem., Int. Ed.* **2006**, *45*, 3488−3491. (c) Frey, G. D.; Lavallo, V.; Donnadieu, B.; Schoeller, W. W.; Bertrand, G. Facile Splitting of Hydrogen and Ammonia by Nucleophilic Activation at a Single Carbon Center. *Science* **2007**, *316*, 439−441. (d) Arrowsmith, M.; Böhnke, J.; Braunschweig, H.; Celik, M. A.; Dellermann, T.; Hammond, K. Uncatalyzed Hydrogenation of First-Row Main Group Multiple Bonds. *Chem.—Eur. J.* **2016**, *22*, 17169−17172.

(4) Chu, J.; Munz, D.; Jazzar, R.; Melaimi, M.; Bertrand, G. Synthesis of Hemilabile Cyclic (Alkyl)(amino)carbenes (CAACs) and Applications in Organometallic Chemistry. *J. Am. Chem. Soc.* **2016**, *138*, 7884−7887.

(5) (a) Munz, D.; Chu, J.; Melaimi, M.; Bertrand, G. NHC-CAAC Heterodimers with Three Stable Oxidation States. *Angew. Chem., Int. Ed.* **2016**, *55*, 12886–12890. (b) Paul, U. S. D.; Radius, U. Ligand versus Complex: C–F and C–H Bond Activation of Polyfluoroaromatics at a Cyclic (Alkyl)(Amino)Carbene. *Chem.—Eur. J.* **2017**, *23*, 3993–4009. (c) Mandal, D.; Dolai, R.; Chrysochos, N.; Kalita, P.; Kumar, R.; Dhara, D.; Maiti, A.; Narayanan, R. S.; Rajaraman, G.; Schulzke, C.; Chandrasekhar, V.; Jana, A. Stepwise Reversible Oxidation of *N*-Peralkyl-Substituted NHC–CAAC Derived Triazaalkenes: Isolation of Radical Cations and Dications. *Org. Lett.* **2017**, *19*, 5605–5608.

(6) For selected references: (a) Zhong, R.; Lindhorst, A. C.; Raba, A.; Högerl, M. P.; Zhong, R.; Lindhorst, A. C.; Groche, F. J.; Kühn, F. E. Immobilization of N-Heterocyclic Carbene Compounds: A Synthetic Perspective. *Chem. Rev.* **2017**, *117*, 1970–2058. (b) Bellemin-Laponnaz, S.; Dagorne, S. Group 1 and 2 and Early Transition Metal Complexes Bearing N-Heterocyclic Carbene Ligands: Coordination Chemistry, Reactivity, and Applications. *Chem. Rev.* **2014**, *114*, 8747–8774. (c) Riener, K.; Herrmann, W. A.; Kühn, F. E. Chemistry of Iron *N*-Heterocyclic Carbene Complexes: Syntheses, Structures, Reactivities, and Catalytic Applications. *Chem. Rev.* **2014**, *114*, 5215–5272. (d) Wang, Y.; Robinson, G. H. Carbene Stabilization of Highly Reactive Main-Group Molecules. *Inorg. Chem.* **2011**, *50*, 12326–12337. (e) Bourissou, D.; Guerret, O.; Gabbaï, F. P.; Bertrand, G. Stable Carbenes. *Chem. Rev.* **2000**, *100*, 39–92.

(7) For selected references: (a) Jana, A.; Majumder, M.; Majumdar, M.; Huch, V.; Zimmer, M.; Scheschkewitz, D. NHC-coordinated silagermenylidene functionalized in allylic position and its behaviour as a ligand. *Dalton Trans.* **2014**, *43*, 5175–5181. (b) Jana, A.; Omlor, I.; Huch, V.; Rzepa, H. S.; Scheschkewitz, D. N-Heterocyclic Carbene Coordinated Neutral and Cationic Heavier Cyclopropylidenes. *Angew. Chem., Int. Ed.* **2014**, *53*, 9953–9956. (c) Cowley, M. J.; Huch, V.; Rzepa, H. S.; Scheschkewitz, D. Equilibrium between a cyclotrisilene and an isolable base adduct of a disilenyl silylene. *Nat. Chem.* **2013**, *5*, 876–879. (d) Jana, A.; Huch, V.; Scheschkewitz, D. NHC-Stabilized Silagermenylidene: A Heavier Analogue of Vinylidene. *Angew. Chem., Int. Ed.* **2013**, *52*, 12179–12182. (e) Mandal, D.; Dhara, D.; Maiti, A.; Klemmer, L.; Huch, V.; Zimmer, M.; Rzepa, H. S.; Scheschkewitz, D.; Jana, A. Mono- and Dicoordinate Germanium(0) as a Four-Electron Donor. *Chem.—Eur. J.* **2018**, *24*, 2873–2878.

(8) (a) Ghadwal, R. S.; Roesky, H. W.; Merkel, S.; Henn, J.; Stalke, D. Lewis Base Stabilized Dichlorosilylene. *Angew. Chem., Int. Ed.* **2009**, *48*, 5683–5686. (b) Filippou, A. C.; Chernov, O.; Schnakenburg, G. SiBr$_2$(Idipp): A Stable N-Heterocyclic Carbene Adduct of Dibromosilylene. *Angew. Chem., Int. Ed.* **2009**, *48*, 5687–5690.

(9) Filippou, A. C.; Lebedev, Y. N.; Chernov, O.; Straßmann, M.; Schnakenburg, G. Silicon(II) Coordination Chemistry: N-Heterocyclic Carbene Complexes of Si^{2+} and SiI$^+$. *Angew. Chem., Int. Ed.* **2013**, *52*, 6974–6978.

(10) Mandal, D.; Dolai, R.; Kalita, P.; Narayanan, R. S.; Kumar, R.; Sobottka, S.; Sarkar, B.; Rajaraman, G.; Chandrasekhar, V.; Jana, A. "Abnormal" Addition of NHC to a Conjugate Acid of CAAC: Formation of *N*-Alkyl-Substituted CAAC. *Chem.—Eur. J.* **2018**, *24*, 12722–12727.

(11) (a) Häller, L. J. L.; Page, M. J.; Erhardt, S.; Macgregor, S. A.; Mahon, M. F.; Naser, M. A.; Vélez, A.; Whittlesey, M. K. Experimental and Computational Investigation of C–N Bond Activation in Ruthenium N-Heterocyclic Carbene Complexes. *J. Am. Chem. Soc.* **2010**, *132*, 18408–18416. (b) Hering, F.; Radius, U. From NHC to Imidazolyl Ligand: Synthesis of Platinum and Palladium Complexes d^{10}-[M(NHC)$_2$] (M = Pd, Pt) of the NHC 1,3-Diisopropylimidazolin-2-ylidene. *Organometallics* **2015**, *34*, 3236–3245. (c) Day, B. M.; Pugh, T.; Hendriks, D.; Guerra, C. F.; Evans, D. J.; Bickelhaupt, F. M.; Layfield, R. A. Normal-to-Abnormal Rearrangement and NHC Activation in Three-Coordinate Iron(II) Carbene Complexes. *J. Am. Chem. Soc.* **2013**, *135*, 13338–

13341. (d) Burling, S.; Mahon, M. F.; Powell, R. E.; Whittlesey, M. K.; Williams, J. M. J. Ruthenium Induced C–N Bond Activation of an N-Heterocyclic Carbene: Isolation of C- and N-Bound Tautomers. *J. Am. Chem. Soc.* **2006**, *128*, 13702–13703. (e) Hu, Y.-C.; Tsai, C.-C.; Shih, W.-C.; Yap, G. P. A.; Ong, T.-G. The Zirconium Benzyl Mediated C–N Bond Cleavage of an Amino-Linked N-Heterocyclic Carbene. *Organometallics* **2010**, *29*, 516–518. (f) Caddick, S.; Cloke, F. G. N.; de K. Lewis, A. K. Unusual Reactivity of a Nickel N-Heterocyclic Carbene Complex: *tert*-Butyl Group Cleavage and Silicone Grease Activation. *Angew. Chem., Int. Ed.* **2004**, *43*, 5824–5827. (g) Liang, Q.; Salmon, A.; Kim, P. J.; Yan, L.; Song, D. Unusual Rearrangement of an *N*-Donor-Functionalized N-Heterocyclic Carbene Ligand on Group 8 Metals. *J. Am. Chem. Soc.* **2018**, *140*, 1263–1266.

(12) Rosas-Sánchez, A.; Alvarado-Beltran, I.; Baceiredo, A.; Hashizume, D.; Saffon-Merceron, N.; Branchadell, V.; Kato, T. The Lightest Element Phosphoranylidene: NHC-Supported Cyclic Borylidene–Phosphorane with Significant B=P Character. *Angew. Chem., Int. Ed.* **2017**, *56*, 4814–4818.

(13) See the Supporting Information for the details of theoretical calculation.

(14) Jigami, T.; Takimiya, K.; Otsubo, T.; Aso, Y. Novel Selenocycle-Fused TTF-Type of Electron Donors Forming Conducting Molecular Complexes: Bis(ethyleneseleno)tetrathiafulvalene (BES-TTF), Diselenolotetrathiafulvalene (DS-TTF), and Bis-(ethyleneseleno)tetraselenafulvalene (BES-TSF). *J. Org. Chem.* **1998**, *63*, 8865–8872.

(15) Zhou, J.; Liu, L. L.; Cao, L. L.; Stephan, D. W. Nitrogen-Based Lewis Acids: Synthesis and Reactivity of a Cyclic (Alkyl)-(Amino)Nitrenium Cation. *Angew. Chem., Int. Ed.* **2018**, *57*, 3322–3326.

(16) Kuhn, N.; Kratz, T. Synthesis of Imidazole-2-Ylidenes by Reduction of Imidazole-2(3h)-Thiones. *Synthesis* **1993**, 561–562.

(17) Bertrand, G.; Lavallo, V.; Canac, Y. Stable Cyclic (Alkyl)-(Amino) Carbenes As Ligands For Transition Metal Catalysts WO Patent 2006138166, 2006.

(18) Frisch, M. J.; Trucks, G. W.; Schlegel, H. B.; Scuseria, G. E.; Robb, M. A.; Cheeseman, J. R.; Scalmani, G.; Barone, V.; Petersson, G. A.; Nakatsuji, H.; Li, X.; Caricato, M.; Marenich, A.; Bloino, J., Janesko, B. G.; Gomperts, R.; Mennucci, B.; Hratchian, H. P.; Ortiz, J. V.; Izmaylov, A. F.; Sonnenberg, J. L.; Williams-Young, D.; Ding, F.; Lipparini, F.; Egidi, F.; Goings, J.; Peng, B.; Petrone, A.; Henderson, T.; Ranasinghe, D.; Zakrzewski, V. G.; Gao, J.; Rega, N.; Zheng, G.; Liang, W.; Hada, M.; Ehara, M.; Toyota, K.; Fukuda, R.; Hasegawa, J.; Ishida, M.; Nakajima, T.; Honda, Y.; Kitao, O.; Nakai, H.; Vreven, T.; Throssell, K.; Montgomery, J. A.; Peralta, J. E., Jr.; Ogliaro, F.; Bearpark, M.; Heyd, J. J.; Brothers, E.; Kudin, K. N.; Staroverov, V. N.; Keith, T.; Kobayashi, R.; Normand, J.; Raghavachari, K.; Rendell, A.; Burant, J. C.; Iyengar, S. S.; Tomasi, J.; Cossi, M.; Millam, J. M.; Klene, M.; Adamo, C.; Cammi, R.; Ochterski, J. W.; Martin, R. L.; Morokuma, K.; Farkas, O.; Foresman, J. B.; Fox, D. J. *Gaussian 09*, Revision A.02; Gaussian, Inc.: Wallingford CT, 2009.

(19) (a) Lee, C.; Yang, W.; Parr, R. G. Development of the Colle-Salvetti correlation-energy formula into a functional of the electron density. *Phys. Rev. B: Condens. Matter Mater. Phys.* **1988**, *37*, 785–789. (b) Stephens, P. J.; Devlin, F. J.; Chabalowski, C. F.; Frisch, M. J. Ab Initio Calculation of Vibrational Absorption and Circular Dichroism Spectra Using Density Functional Force Fields. *J. Phys. Chem.* **1994**, *98*, 11623–11627.

(20) (a) Schäfer, A.; Huber, C.; Ahlrichs, R. Fully optimized contracted Gaussian basis sets of triple zeta valence quality for atoms Li to Kr. *J. Chem. Phys.* **1994**, *100*, 5829–5835. (b) Schäfer, A.; Horn, H.; Ahlrichs, R. Fully optimized contracted Gaussian basis sets for atoms Li to Kr. *J. Chem. Phys.* **1992**, *97*, 2571–2577.

(21) Neese, F. Software update: the ORCA program system, version 4.0. *Wiley Interdiscip. Rev.: Comput. Mol. Sci.* **2018**, *8*, No. e1327.

(22) Barone, V.; Cossi, M. Quantum calculation of molecular energies and energy gradients in solution by a conductor solvent model. *J. Phys. Chem. A* **1998**, *102*, 1995−2001.

(23) (a) Grimme, S. Semiempirical GGA-type density functional constructed with a long-range dispersion correction. *J. Comput. Chem.* **2006**, *27*, 1787−1799. (b) Grimme, S. Accurate description of van der Waals complexes by density functional theory including empirical corrections. *J. Comput. Chem.* **2004**, *25*, 1463−1473. (c) Grimme, S.; Antony, J.; Ehrlich, S.; Krieg, H. A consistent and accurate ab initio parametrization of density functional dispersion correction (DFT-D) for the 94 elements H-Pu. *J. Chem. Phys.* **2010**, *132*, 154104. (d) Grimme, S.; Ehrlich, S.; Goerigk, L. Effect of the damping function in dispersion corrected density functional theory. *J. Comput. Chem.* **2011**, *32*, 1456−1465.

(24) (a) Perdew, J. P. Erratum: Density-functional approximation for the correlation energy of the inhomogeneous electron gas. *Phys. Rev. B: Condens. Matter Mater. Phys.* **1986**, *34*, 7406. (b) Perdew, J. P. Density-functional approximation for the correlation energy of the inhomogeneous electron gas. *Phys. Rev. B: Condens. Matter Mater. Phys.* **1986**, *33*, 8822. (c) Becke, A. D. Density-functional exchange-energy approximation with correct asymptotic behaviour. *Phys. Rev. A: At., Mol, Opt. Phys.* **1988**, *38*, 3098.

(25) (a) Petrenko, T.; Kossmann, S.; Neese, F. Efficient time-dependent density functional theory approximations for hybrid density functionals: Analytical gradients and parallelization. *J. Chem. Phys.* **2011**, *134*, 054116. (b) Neese, F.; Olbrich, G. Efficient use of the resolution of the identity approximation in time-dependent density functional calculations with hybrid density functionals. *Chem. Phys. Lett.* **2002**, *362*, 170−178. (c) Izsák, R.; Neese, F. An overlap fitted chain of spheres exchange method. *J. Chem. Phys.* **2011**, *135*, 144105. (d) Whitten, J. L. Coulombic potential energy integrals and approximations. *J. Chem. Phys.* **1973**, *58*, 4496−4501. (e) Vahtras, O.; Almlöf, J.; Feyereisen, M. W. Integral approximations for LCAO-SCF calculations. *Chem. Phys. Lett.* **1993**, *213*, 514−518. (f) Neese, F.; Wennmohs, F.; Hansen, A.; Becker, U. Efficient, approximate and parallel Hartree−Fock and hybrid DFT calculations. A 'chain-of-spheres' algorithm for the Hartree−Fock exchange. *Chem. Phys.* **2009**, *356*, 98. (g) Neese, F. An improvement of the resolution of the identity approximation for the formation of the Coulomb matrix. *J. Comput. Chem.* **2003**, *24*, 1740.

(26) (a) Eichkorn, K.; Treutler, O.; Öhm, H.; Häser, M.; Ahlrichs, R. Auxiliary basis sets to approximate Coulomb potentials. *Chem. Phys. Lett.* **1995**, *242*, 652−660. (b) Eichkorn, K.; Weigend, F.; Treutler, O.; Ahlrichs, R. Auxiliary basis sets for main row atoms and transition metals and their use to approximate Coulomb potentials. *Theor. Chem. Acc.* **1997**, *97*, 119−124.

(27) Staroverov, V. N.; Scuseria, G. E.; Tao, J.; Perdew, J. P. Comparative assessment of a new nonempirical density functional: Molecules and hydrogen-bonded complexes. *J. Chem. Phys.* **2003**, *119*, 12129−12137.

(28) Barone, V. In *Recent Advances In Density Functional Methods, Part I*; Chong, D. P., Ed.; World Scientific: Singapore, 1997.

(29) (a) Hanwell, M. D.; Curtis, D. E.; Lonie, D. C.; Vandermeersch, T.; Zurek, E.; Hutchison, G. R. Avogadro: an advanced semantic chemical editor, visualization, and analysis platform. *J. Cheminform.* **2012**, *4*, 17. (b) *Avogadro*, an open-source molecular builder and visualization tool. Version 1.2.0 (2016). Modified Version with Extended ORCA Support. http://avogadro.openmolecules.net/ and https://orcaforum.cec.mpg.